Biophysical Chemistry, 37 (1990) 323–340
Elsevier

BIOCHE 01490

Comparative least-squares analysis of hemoglobin oxygen equilibrium curves

David Myers [a], Kiyohiro Imai [b] and Takashi Yonetani [a]

[a] *Department of Biochemistry and Biophysics, University of Pennsylvania School of Medicine, Philadelphia, PA 19104, U.S.A.*
and [b] *Department of Physico-Chemical Physiology, Medical School, Osaka University, Osaka 530, Japan*

Received 15 January 1990
Revised manuscript received 13 March 1990
Accepted 13 March 1990

Hemoglobin; Oxygen binding; Adair equation; Triply liganded species

The oxygen-binding properties of hemoglobin have been studied at 600 μM protein concentration with organic phosphate, and analyzed by a series of different nonlinear least-squares analysis methods to determine whether reports of negligibly small values of the third overall Adair parameter, A_3, are consequences of the data or a product of the data analysis. Data from other laboratories were analyzed as well. The single most important factor in creating a measurement that yields a small A_3 is the use of equally weighted fitting in the Adair equation, while end-weighted fitting generally yields a larger A_3. Endpoint extrapolation is ruled out as a major cause of abnormal A_3 values. Monte Carlo simulations of the 600 μM results suggest that, if a small A_3 were present, end weighting is at least as sensitive to a small A_3 as equal weighting. We conclude that equally weighted fitting of the tetrameric Adair equation is unable to resolve the upper asymptote of the oxygen-binding data, resulting in an unusually small value for A_3.

1. Introduction

The study of hemoglobin oxygenation has been the focus of a large body of research over many years, and in 1925, Adair suggested that the binding of oxygen to hemoglobin could be described by four consecutive binding steps, each step binding a single oxygen [1,2]. The equation that resulted from this mechanism, the Adair equation, can be expressed in terms of the overall binding parameters:

$$Y=\frac{A_1p+2A_2p^2+3A_3p^3+4A_4p^4}{4\left(1+A_1p+A_2p^2+A_3p^3+A_4p^4\right)}$$

or as stepwise binding parameters:

$$Y=\left(K_1p+3K_1K_2p^2+3K_1K_2K_3p^3+K_1K_2K_3K_4p^4\right)/\left(1+4K_1p+6K_1K_2p^2+4K_1K_2K_3p^3+K_1K_2K_3K_4p^4\right)$$

where Y denotes the fractional saturation of the hemoglobin molecule, p is the partial pressure of oxygen, and the stepwise binding parameters are related to the overall parameters by the relationships

$A_1=4K_1$, $A_2=6K_1K_2$, $A_3=4K_1K_2K_3$, and $A_4=K_1K_2K_3K_4$.

In 1955, Roughton and his co-workers [3] became the first researchers to collect sufficient hemoglobin oxygen equilibrium data of accuracy high enough to resolve the four Adair parameters, finding all four to be positive. In 1968, Imai and his co-workers [4–9] introduced the automatic re-

Correspondence address: T. Yonetani, Department of Biochemistry and Biophysics, University of Pennsylvania School of Medicine, Philadelphia, PA 19104, U.S.A.

Abbreviations: Hb, hemoglobin; metHb, methemoglobin; IHP, inositol hexaphosphate; DPG, 2,3-diphosphoglycerate; OEC, oxygen equilibrium curve; CoHb, cobalt hemoglobin; ΔA_t, total absorbance change during an OEC experiment; $\sigma_{\Delta A_t}$, the standard error of the total absorbance change; ΔA, the change in absorbance observed with one thin-layer cell measurement.

cording method. It was fast, accurate, reproducible, and consistently yielded positive Adair parameters.

In a series of papers, Gill and his co-workers [10–16] have suggested that the third overall Adair parameter was essentially zero, a value that implies a vanishingly small amount of the triply ligated tetramer species. In support of their observations, three hypotheses were presented. First, the thin-layer cell of Dolman and Gill [17] was supposed to produce intrinsically superior data to other methods. Second, the data recorded by the thin-layer cell were not influenced by dimer formation, and dimers could be neglected. Third, the positive results of Imai et al. were caused by dimer formation, or these results were a product of poorly chosen end points.

The first hypothesis, that data from the thin-layer cell are intrinsically superior, appears to ignore the fact that Gill and co-workers measure fairly small total absorbance changes (0.1–0.2) with a small number of data points. As a result, the spectrophotometric signal-to-noise ratio suffers when compared to other methods. Moreover, the number of points taken is fixed by the thin-layer cell itself, and cannot be easily increased. In contrast, the Imai cell has seldom been used to its physical limits. Imai cell deoxygenation experiments are readily performed with reoxygenation as a probe of reproducibility, and taking several hundred points should be straightforward, since points will be collected several seconds apart and thus each point represents an independent measurement.

As point counts are increased, the signal-to-noise ratio increases by the inverse square root of the number of points. Hypothetically, as the number of points grows larger, a limit could be reached where the solution to a tetrameric Adair equation becomes effectively independent of the method chosen for analyzing the data. We were interested in determining whether such an effect could be observed.

The second hypothesis, that the tetrameric Adair parameters derived from thin-layer analysis were not influenced by dimer formation, is probably true. The third hypothesis was examined in part by Imai and Yonetani [7], who demonstrated that the tetrameric Adair parameters obtained from Imai cell data were relatively consistent over a range of protein concentrations from 60 μM to 1 mM, and thus dimers were not a crippling factor in the parameters obtained. Moreover, the hemoglobin concentration dependences measured under these conditions did not indicate a small A_3 at high protein concentrations. The issue of end-points will be addressed in this paper.

Our postulate was that the differences in Adair parameters would be revealed through different data analysis techniques. Considering that both Di Cera and Gill [13] and Imai et al. [7,18] have measured oxygen equilibrium curves of human adult hemoglobin (HbA) with IHP under nearly identical conditions, and that their results are markedly different with respect to the third overall Adair parameter, the probability that an experimental perturbation could yield the differences in Adair parameters is small. Now Gill and co-workers [10] use equally weighted curve fitting while Imai [5,7] uses end-weighted curve fitting. When this study began, no comparative studies of the effects of weights or the absence of weights had been performed, and thus the differential effects of weighting had not been assessed (during the preparation of this manuscript, however, other comparative studies appeared [19]).

We have measured oxygen equilibrium curves at high concentration (600 μM) in the presence of 5 mM organic phosphates, either DPG or IHP. The data were analyzed by one of four curve-fitting methods, so that comparative analyses were available. Monte Carlo studies were then used to determine whether a simple tetrameric model could resolve the effects on curve-fitting parameters of the data. Data sets from other laboratories were also analyzed in an attempt to determine whether differences were in the data or perhaps in the analysis.

2. Materials and methods

HbA was obtained from washed red blood cells and stored in liquid nitrogen in 0.05 M Hepes, containing 0.1 M NaCl, until ready for use. The components of the met-Hb reducing system [20], DPG, and IHP were purchased from Sigma. All other chemicals were of reagent grade.

Oxygen equilibrium curves were recorded (at the University of Pennsylvania, unless otherwise stated) using the automatic recording system [8] which used a Cary 118C spectrophotometer interfaced to an IBM personal computer. Data were initially analyzed as described by Imai and Yonetani [7,9]. Absorption measurements were taken at pressure intervals defined (during deoxygenation) by the equation $p_i = p_0 \Lambda^i$, where p_0 and p_i denote the original and the i-th pressure measurement, respectively, and the scale factor Λ ($\Lambda \equiv p_{i+1}/p_i$, and $\Lambda < 1.0$) determined the spacing of the points. Absorption measurements taken during the course of the experiment were converted to Y values by the transformation

$$Y = \frac{A_{\text{exp}} - A_{\text{deo}}}{A_{\text{oxy}} - A_{\text{deo}}}$$

where the endpoints, A_{oxy} and A_{deo}, were determined by quadratic extrapolation from Y vs $1/p$ and Y vs p plots, respectively.

A program, FITDABS, was written that could solve the Adair equation using end weighting or equal weighting (these two types of weighting are also described as weighted and unweighted fitting, respectively). The same curve-fitting routine could place simple bounds on fitting parameters. FITDABS also allowed for fits with the endpoints either fixed or floating. Three or four curve-fitting algorithms were tested, and all yielded essentially the same results. The algorithm finally selected was chosen because it was globally convergent and easy to use [21,22]. When this new program fitted data (endpoints fixed, weighted fitting) that had been solved by the Imai program [5,6], the two agreed to three significant digits in the sum of squared residuals and every Adair parameter.

When data were obtained from other laboratories, typically the endpoints had already been calculated, and these data were solved directly by FITDABS without endpoint extrapolation. A version of FITDABS was modified to solve equilibrium curves where ΔA values were input rather than absolute absorbance. This version, FITDABS2, could analyze the absorbance differences, or sum the data and analyze the resultant absolute absorption curve. FITDABS2 was used to analyze the data of refs 14–16.

For the purposes of simulation, noise in the OEC measurement can come from one of two sources, the spectrophotometer, or the reading of the oxygen electrode. Spectrophotometric noise was simulated by a linear noise source resulting in $\sigma_Y = 0.00037\Phi$, where Φ is a Gaussian noise generator with a variance of 1 [19]. The value 0.00037 is derived from the standard spectrophotometric error of a Cary 118C instrument ($\sigma_{\text{abs}} = 0.00022$) divided by the typical absorption change in an Imai cell, 0.6 [7,24]. Pressure error was simulated by setting σ_Y equal to $0.08Y(1-Y)\Phi$ [5]. Pressure error, absorbance error, or the combination of both were used in the simulations.

Trial simulation studies used a program to calculate saturation functions and add Gaussian pressure or absorbance noise. The program then multiplied the data set by 0.6, and a small positive correction was then added, so that all the data were positive valued. The resultant curve was then analyzed as before [9], and then with the new curve-fitting program.

Monte Carlo simulations [23] were performed by a modified version of the data analysis software. Floating endpoints were used throughout the simulations, and the parameter values chosen for simulation were all derived with endpoints floating. No attempt was made to carry out Monte Carlo studies of hand-chosen endpoints, because the volume of data would be too great for an individual to handle. Also, the methods for selecting endpoints, because of the need for interactive interpretation of results, are extremely difficult to automate.

3. Results

Trial simulations of saturation curves with pressure error, using an arbitrary choice of Adair parameters ($K_1 = 0.025$, $K_2 = 0.05$, $K_3 = 0.1$, $K_4 = 4.0$), suggested that a Λ value of 0.90 was insufficient to eliminate weighting dependences in the data. Several unweighted data fittings (ΔA_t floating) with zero-valued overall Adair parame-

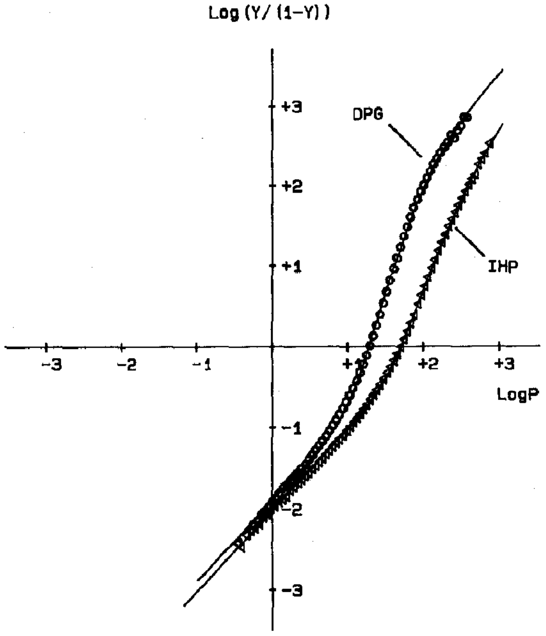

Fig. 1.

Table 1

Solutions to the Adair equation of data in fig. 1

The data were fitted using end weighting or equal weighting, and with endpoints floating or fixed. Note that end-weighted fits all have positive K_3, while equally weighted fits have $A = 0.0$. P_m, median pressure (in Torr); N_{max}, maximum Hill coefficient; σ, standard error of the curve fit. Adair parameters for 600 μM oxygen equilibrium data in the presence of 5 mM organic phosphate. Buffer was 0.05 M Hepes, 0.1 M Cl^-, pH 7.4; $t = 20°$C.

	DPG	IHP
Weighted, fixed		
K_1 (Torr^{-1})	0.012965	0.009712
K_2 (Torr^{-1})	0.0077489	0.008034
K_3 (Torr^{-1})	0.042054	0.003497
K_4 (Torr^{-1})	2.6037	0.98319
P_m (Torr)	17.4	42.7
N_{max}	3.00	2.414
σ	2.40×10^{-5}	2.62×10^{-5}
Points	313	358
Weighted, ΔA_t floating		
K_1 (Torr^{-1})	0.014714	0.008902
K_2 (Torr^{-1})	0.0088728	0.011471
K_3 (Torr^{-1})	0.017362	0.001164
K_4 (Torr^{-1})	5.0804	2.5376
P_m (Torr)	17.2	42.7
σ	1.57×10^{-5}	1.91×10^{-5}
Unweighted, fixed		
A_1 (Torr^{-1})	0.058642	0.035350
A_2 (Torr^{-2})	0.0011722	0.001172
A_3 (Torr^{-3})	0.0	0.0
A_4 (Torr^{-4})	1.09×10^{-5}	3.01×10^{-7}
P_m (Torr)	17.4	42.7
σ	3.77×10^{-3}	1.87×10^{-3}
Unweighted, ΔA_t floating		
A_1 (Torr^{-1})	0.072634	0.034402
A_2 (Torr^{-2})	0.001005	0.000693
A_3 (Torr^{-3})	0.0	0.0
A_4 (Torr^{-4})	1.20×10^{-5}	2.96×10^{-7}
P_m (Torr)	17.0	42.9
σ	3.18×10^{-3}	1.83×10^{-3}

ters were obtained in a total collection of 20 simulations. When the A value was increased to 0.98, however, zero-valued fittings of the simulations disappeared, suggesting that at this point density, pressure error would no longer be a major contributor to zero-value determinations. In these initial simulations, absorbance error was not a major contributor to zero values at $A = 0.90$. Consequently, all the data presented from the University of Pennsylvania were collected at $A = 0.98$ or larger.

Two asymptotes of slope less than 2.0 are observed in the Hill plot of a 600 μM hemoglobin solution in 5 mM DPG (fig. 1; see also appendix A). The weighted and unweighted solutions to fig. 1 are listed in table 1, with weighted solutions yielding a positive K_3 and unweighted solutions giving a zero A_3 *. The results for 5 mM IHP are similar to those for 5 mM DPG, with the exception that, because of the large P_m of IHP, an upper asymptote with a slope of unity is not seen with the IHP data.

It is interesting to note that the solutions obtained by different weighting methods are different, despite pains taken to maximize the equivalence of the methods. All fits were performed on the same data set, with the same initial choice of

---

* Throughout this paper, the zero A implies that it could be negative or truly zero if it was floated and unbound during the least-squares fitting iterations, and then the values of the other A terms could be different from those listed in the relevant tables.

Table 2

The effects of incomplete high Torr data on the resolution of K_4

Data points were removed from the IHP data file of fig. 1 and the Adair coefficients calculated to determine effects of loss of high pressure data on calculation of K_4. The value of K_4 (weighted fitting) with 600 μM HbA + 5 mM IHP data, as maximum Torr value analyzed is varied.

Torr	K_4 (ΔA_t floating)	K_4 (fixed)	Points
760	2.60	0.983	358
700	3.05	0.983	355
650	3.54	0.984	352
625	4.21	0.980	350
600	170.51	0.951	347

endpoints, a large number of data points, and the same fitting program. It is also important to point out that the nonzero values could not have been caused by poor endpoint selection alone, otherwise the curve-fitting procedures with endpoints floating would both yield zero values and those with fixed endpoints nonzero. Moreover, as the oxygen saturation is measured in wider ranges, the ability of endpoint choice to affect the fitting parameters should diminish (table 2).

Data from other laboratories were analyzed by comparative methods as well, in order to see whether the trends we observed were unique to our data or common to many different sets of data. Before proceeding, it should be borne in mind that researchers cannot anticipate having data sets tested under a wide variety of conditions other than those they personally have chosen. Data sets that are optimal for one particular fitting technique may not be optimal for others. The most important consideration is the comparative trends, which we believe show a strong dependence of $A_3 = 0$ results on unweighted fitting.

3.1. Comparison with data from other laboratories

3.1.1. Vandegriff et al.

Vandegriff et al. [25,26] had reported that data from HbA had an $A_3 = 0$, whereas data from α-α cross-linked hemoglobins did not. Vandegriff et al. used a six-parameter, unweighted fitting technique. We obtained two data sets from this laboratory, fitting being performed using weighted and unweighted techniques. While weighted fitting of their data yielded an $A_2 = 0$ *, two clearly defined unity asymptotes were observed in these data. The protein concentration used in their experiments was 200 μM.

3.1.2. M. Fujii

M. Fujii is a researcher in our laboratory, and he gave us 11 data sets, with endpoints chosen, for comparative data analysis. The buffer used was 0.05 M Tris, 0.1 M Cl^-, pH ranged from 8.0 to 6.8, and the hemoglobin concentration was 60 μM. All data sets had positive A_3 values when fitted with weights, while eight of the 11 yielded an $A_3 = 0$ when fitted without weights, and two others had enlarged, unresolved K_4 values **.

3.1.3. Poyart and co-workers

C. Poyart sent six HbA data sets for analysis. Three of these sets were of low cooperativity ($n \approx 2.0$), while the remaining three were highly cooperative ($n \geq 2.8$). None of the data sets at low cooperativity exhibited any kind of A_3 effects, while two of the three highly cooperative data sets had a zero A_3 when analyzed using equal weights.

3.1.4. Chu et al.

Data at pH 7.4 from the data sets of Chu et al. [27] clearly exhibited trends in the unweighted direction (table 3 (A)). All unweighted fits either yielded an $A_3 = 0$, or clearly enlarged and unresolved K_4 values, whereas none of the data exhibited an $A_3 = 0$ when fitted with weights. Because of the low concentrations of these samples, the $A_3 = 0$ values were attributed to dimer effects on the tetrameric Adair equation, while Chu et al. extracted positive dimer and tetramer coefficients via fitting to a tetramer-dimer linkage scheme.

---

* Since Vandegriff et al. collected data for equal increments of time, and our analysis procedure is optimized for data collected in equal units of log pressure, this $A_2 = 0$ value is probably an artifact.

** An unresolved parameter is one for which the standard error is larger than the parameter itself.

Table 3

Comparative analysis of OEC data from other laboratories

Sets A–E were obtained with endpoints chosen. These values for A_{oxy} and A_{deo} were kept as initial values in our curve fitting. (A) Data sets from Chu et al. [27] at pH 7.4. Since the values in ref. 27 were optimized for a dimer-tetramer fit, the appearance of $A_2 = 0$ values in these weighted fits should not be construed as being a product of a poor data set. The small, positive A_3 value in the unweighted fitting of the 14.1 μM set from Chu et al. has a relative error of 158%. (B) Data sets from K. Imai. Buffers used were 0.05 M Bis-Tris, 0.1 M Cl$^-$, pH 7.4. (C) Data sets from Gill and co-workers. Set F from the 71.6 Torr CO$_2$ data set from Doyle et al. [15] and set G from the data set of Di Cera and Gill [13]. Set G has a relative error of 183% in its weighted A_3 value. The weighted values of the Adair parameters in set G bear a substantive resemblance to the Adair parameters of the IHP data in table 1.

Laboratory	Data set	Weighted	Unweighted
(A) Chu et al.	Set A		
	A_1 (Torr^{-1})	0.15440	0.21307
	A_2 (Torr^{-2})	0.07258	0.01293
	A_3 (Torr^{-3})	0.00117	0.0
	A_4 (Torr^{-4})	0.00218	0.00248
	P_m (Torr)	4.63	4.48
	N_{max}	3.059	3.027
	σ	6.17×10^{-5}	3.02×10^{-3}
	Concentration (μM)	5.15	
	Points	67	
	Set B		
	A_1 (Torr^{-1})	0.15192	0.21375
	A_2 (Torr^{-2})	0.00	0.00717
	A_3 (Torr^{-3})	0.00246	0.00033
	A_4 (Torr^{-4})	0.00160	0.00182
	P_m (Torr)	5.00	4.84
	N_{max}	3.004	3.097
	σ	7.68×10^{-5}	2.49×10^{-3}
	Concentration (μM)	14.1	
	Points	69	
(B) K. Imai	Set C		
	A_1 (Torr^{-1})	0.33107	0.32929
	A_2 (Torr^{-2})	0.02452	0.05370
	A_3 (Torr^{-3})	0.00516	0.0
	A_4 (Torr^{-4})	0.00663	0.00671
	P_m (Torr)	3.50	3.49
	N_{max}	2.696	2.681
	σ	4.92×10^{-5}	3.60×10^{-3}
	Concentration (mM)	1.2	
	Points	56	
	Set D		
	A_1 (Torr^{-1})	0.32764	0.33443
	A_2 (Torr^{-2})	0.02108	0.04594
	A_3 (Torr^{-3})	0.00486	0.0
	A_4 (Torr^{-4})	0.00717	0.00723
	P_m (Torr)	3.44	3.49
	N_{max}	2.778	2.761
	σ	4.32×10^{-5}	4.03×10^{-3}
	Concentration (mM)	1.2	
	Points	56	
	Set E		
	A_1 (Torr^{-1})	0.10836	0.13675

(continued)

Table 3 (continued)

Laboratory	Data set	Weighted	Unweighted
(B) K. Imai	Set E		
	A_2 (Torr^{-2})	0.00704	0.01623
	A_3 (Torr^{-3})	0.00260	0.0
	A_4 (Torr^{-4})	0.00301	0.00303
	P_m (Torr)	4.27	4.26
	N_{max}	3.125	3.101
	σ	1.59×10^{-4}	5.14×10^{-3}
	Concentration (μM)	60	
	Points	48	
(C) Gill and co-workers	Set F	Weighted A fit	Unweighted ΔA fit
	A_1 (Torr^{-1})	0.19307	0.10247
	A_2 (Torr^{-2})	0.00000	0.00187
	A_3 (Torr^{-3})	0.00000	0.0
	A_4 (Torr^{-4})	4.20×10^{-4}	6.69×10^{-5}
	P_m (Torr)	6.98	11.06
	ΔA_t	0.0728	0.0735
	σ	6.56×10^{-6}	1.76×10^{-3}
	Concentration (mM)	4	
	Points	19	
	Set G		
	A_1 (Torr^{-1})	0.02066	0.01904
	A_2 (Torr^{-2})	3.20×10^{-4}	3.36×10^{-4}
	A_3 (Torr^{-3})	1.02×10^{-6}	0.0
	A_4 (Torr^{-4})	7.78×10^{-8}	7.58×10^{-8}
	P_m (Torr)	59.89	60.3
	ΔA_t	0.1974	0.1972
	σ	4.82×10^{-5}	5.35×10^{-4}
	Concentration (mM)	2	
	Points	15	

3.1.5. K. Imai

Three of four data sets previously obtained by K.I. exhibited an $A_3 = 0$ when fitted using unweighted methods, while none exhibited $A_3 = 0$ when fitted by weighted methods (table 3 (**B**)). The single data set that did not exhibit this trend was collected by hand; the others were collected by computer. The protein concentration ranged from 60 μM to 1.2 mM.

3.1.6. Gill, Doyle et al. and ΔA fitting methods

Seven sets of thin-layer data were received from M. Doyle [15,16] and analyzed. Another published data set [13,19] was analyzed as well (table 3 (C)). When solved by methods similar to Gill's (unweighted fitting to ΔA measurements), the parameters obtained were slightly different, but within the standard errors of the published values. An unexpected discovery was small positive unresolved A_3 values in three of the data sets, since the published data from Gill's laboratory since 1987 have exhibited only $A_3 = 0$ results. Weighting a ΔA equation led to solutions where the first three overall Adair parameters were zero, and only A_4 was resolved. Summing the ΔA values and fitting the saturation curve directly led to slightly different fits when data were equally weighted, although whether the differences between the ΔA and sum of ΔA fits were significant was hard to tell with five data sets. The weighted fits of the summed form of the data yielded an $A_2 = 0$ and an $A_3 = 0$ in five of the eight sets. The exceptions had IHP as an allosteric effector, and a ΔA_t of 0.19–0.29 absorbance units, about 2–3-times larger than those of the other data sets. The large ΔA_t may have been significant in the ability of the weighted technique to resolve the Adair parameters. Interestingly, the values of the weighted Adair parameters of the IHP data set in table 3 (C) compare reasonably well with the values obtained with IHP in table 1.

Data from our laboratory were taken and converted to ΔA or difference form. The results with $\Lambda = 0.98$ were unsatisfactory, while removing points unitl $\Lambda = 0.90$ produced resolvable fittings. Data that yielded a nonzero A_3 by weighted fitting clearly exhibited a zero A_3 when analyzed by unweighted ΔA methods. Tests with ΔA and other fitting methods suggest that the probability of obtaining a small A_3 value is ordered in the following way:

$$5 \text{ diff} > 6 \text{ unw} \geq 4 \text{ unw} \gg 6 \text{ wei} \geq 4 \text{ wei},$$

where diff denotes ΔA fitting, and wei and unw are weighted and unweighted fitting, respectively; 4–6 refer to the number of independently variable parameters in the curve fitting.

3.2. $\sigma_{\Delta A_t}$ *and the number of data points*

Marden et al. [28] have pointed out that the standard deviation of ΔA_t in the data of Gill et al. is large (approx. 0.5%), so large that their data, despite the small A_3 values, could conceivably accommodate solutions where A_3 is essentially normal. Independent checks in our laboratory confirm that a 0.5% change in ΔA_t could induce this kind of effect, and in fact, changes smaller than 0.2% in ΔA_t can often completely alter the overall Adair parameters. Since $\sigma_{\Delta A_t}$ for unweighted fitting is larger than $\sigma_{\Delta A_t}$ for weighted fitting (fig. 2), we calculated the $\sigma_{\Delta A_t}$ for a variety of data sets using unweighted fitting. We then

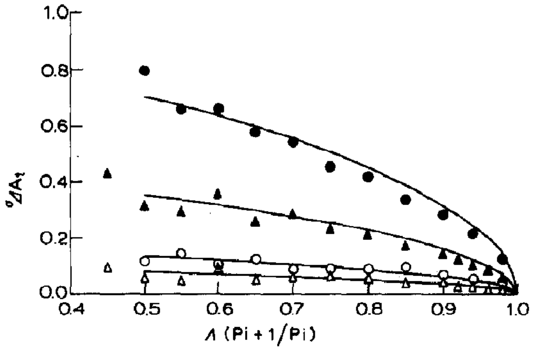

Fig. 2.

Table 4

Variation of $\sigma_{\Delta A_t}$ with alteration in number of analyzed data points

The data sets in fig. 1 were taken, points were removed from the data files, and the Adair coefficients were calculated for six-parameter fitting. The $\sigma_{\Delta A_t}$ values obtained in this way were fitted to the equation $\sigma_{\Delta A_t} = cN^{-1/2}$, where $\sigma_{\Delta A_t}$ is expressed as a percentage relative to the total absorbance change, c is a variable parameter, and N is the number of OEC data points. Fitted values of c were: 5 mM DPG weighted had $\sigma_{\Delta A_t} = (0.482 \pm 0.014)N^{-1/2}$, 5 mM DPG unweighted had $\sigma_{\Delta A_t} = (2.541 \pm 0.039)N^{-1/2}$, 5 mM IHP weighted had $\sigma_{\Delta A_t} = (0.299 \pm 0.011)N^{-1/2}$, 5 mM IHP unweighted had $\sigma_{\Delta A_t} = (1.349 \pm 0.028)N^{-1/2}$.

Λ	N	Weighting	
		End	Equal
		$\sigma_{\Delta A_t}$ (%)	$\sigma_{\Delta A_t}$ (%)
5 mM DPG			
0.98	313	0.038	0.123
0.94	105	0.052	0.214
0.90	63	0.066	0.283
0.85	45	0.095	0.336
0.80	32	0.087	0.417
0.75	27	0.090	0.453
0.70	21	0.087	0.543
0.65	19	0.123	0.577
0.60	16	0.104	0.661
0.55	15	0.143	0.658
0.50	13	0.117	0.795
5 mM IHP			
0.98	358	0.017	0.062
0.96	179	0.021	0.087
0.94	120	0.028	0.107
0.92	90	0.027	0.124
0.90	72	0.042	0.146
0.85	52	0.038	0.175
0.80	36	0.055	0.215
0.75	30	0.065	0.233
0.70	24	0.061	0.290
0.65	22	0.051	0.263
0.60	18	0.094	0.360
0.55	17	0.051	0.298
0.50	15	0.060	0.318
0.45	14	0.096	0.433

fitted the values to the function $\eta = aN^{-b}$, where $\eta = 100\sigma_{\Delta A_t}/\Delta A_t$, and N is the number of OEC data points. The fitted values were $a = 0.61 \pm 0.21$, and $b = -0.61 \pm 0.12$, and were consistent with the notion that the accuracy of the endpoints increases in proportion to the inverse square root of N.

Another test of the effects of differing number of data points on the $\sigma_{\Delta A_t}$ values was performed by removing points from the sets of data in table 1. The resulting files were then analyzed for Adair parameters and $\sigma_{\Delta A_t}$. Next, the calculated $\sigma_{\Delta A_t}$ values were fitted to the equation $\sigma_{\Delta A_t} = cN^{-1/2}$ (fig. 2 and table 4). The results from these analyses clearly show that end-weighted fitting resolves the total absorbance change with considerably greater precision than does equally weighted fitting.

3.3. *pH effects and the probability of obtaining small A_3*

Ten data sets obtained in a pH range from 9.0 to 5.8 by K.I. in Osaka University were analyzed by comparative methods (table 5). The results obtained were consistent with the prior data. Interestingly, at pH values of 7.8 or higher, the tendency for equally weighted fitting to yield a small A_3 value disappeared. The shift in T- to R-state transition (i_s) from the third to second oxygenation step at high pH values increases the relative population of triply ligated species, raising the probability of obtaining positive A_3 values. When data were converted to difference form and solved by ΔA methods, all data sets yielded zero A_3 values when analyzed by equally weighted fitting.

3.4. *Cobalt hemoglobin*

Three data sets of CoHb data, and 20 older data sets of CoHb oxygenation (previously measured by Imai et al.) were analyzed for comparative data analysis effects. The protein concentration for these sets ranged from 60 μM to over 400 μM. There were no major differences between the different fitting methods, with some sets yielding the same parameters irrespective of how they were solved, and others being affected by a factor of 2 or 3 by the method of curve fitting. Regardless of the curve-fitting method, there was a positive A_3 found throughout the data analysis.

3.5. *Monte Carlo studies of measurement error*

Do the measurement error terms, which weights correct for, actually cause the differences between the observed Adair parameters? Monte Carlo

Table 5

Variation of overall Adair coefficients with pH using end-weighted and equally weighted fitting with four variable parameters

Data were from Imai (unpublished results). Concentration of protein was 180 μM. The term '*n/a*' was used when the overall Adair coefficient was zero. The results at high pH are notable in that they do not exhibit a small A_3.

pH	End weighted				Equally weighted			
	log A_1	log A_2	log A_3	log A_4	log A_1	log A_2	log A_3	log A_4
0.05 M Tris, 0.1 M Cl$^-$								
9.0	−0.20	−1.28	−0.99	−0.84	−0.20	−0.80	−1.24	−0.83
8.6	−0.06	−1.13	−0.98	−0.79	−0.05	−0.85	−1.16	−0.78
7.8	−0.44	−1.22	−1.56	−1.47	−0.36	−0.91	−2.48	−1.46
7.5	−0.42	−1.67	−2.28	−2.02	−0.40	−1.30	*n/a*	−2.01
7.4	−0.36	−1.86	−2.22	−2.10	−0.37	−1.32	*n/a*	−2.09
0.05 M Bis-Tris, 0.1 M Cl$^-$								
7.4	−0.46	−1.78	−2.13	−2.06	−0.42	−1.29	*n/a*	−2.05
7.0	−0.75	−1.90	−3.11	−2.90	−0.68	−1.79	*n/a*	−2.90
6.6	−1.09	−2.49	−3.71	−3.83	−0.98	−2.33	*n/a*	−3.83
6.2	−1.15	−2.61	−4.37	−4.34	−1.07	−2.51	*n/a*	−4.35
5.8	−1.11	−2.46	−4.47	−4.39	−1.01	−2.47	*n/a*	−4.40

Table 6

Monte Carlo simulations of the DPG and IHP data (fig. 1) under different noise conditions

100 simulations were analyzed for each particular set of conditions studied. Mean, standard deviation, and median values are given. Zeros are the number of intrinsic Adair coefficients with zero-valued parameters encountered. Average σ is the average standard error for the curve fits. DPG simulations: (A) absorbance noise; (B) pressure noise; (C) pressure+absorbance noise. IHP simulations: (D) absorbance noise; (E) pressure noise; (F) pressure+absorbance noise. Noise definitions are given in section 2.

		True	Mean ± S.D.	Median	Zeros
(A) 5 mM DPG, absorbance noise	Weighted fitting	K_1 0.01471	0.01507 ± 0.00092	0.01500	$A_1 = 0$
		K_2 0.00887	0.00712 ± 0.00394	0.00770	$A_2 = 12$
		K_3 0.01736	0.03503 ± 0.03240	0.02677	$A_3 = 5$
		K_4 5.0804	3.0539 ± 2.2692	3.715	$A_4 = 0$
		Trials = 100	av. $\sigma = 1.69\times10^{-5}$		tot. = 17
	Unweighted fitting	K_1 0.01471	0.01472 ± 0.00007	0.01472	$A_1 = 0$
		K_2 0.00887	0.00885 ± 0.00021	0.00881	$A_2 = 0$
		K_3 0.01736	0.01751 ± 0.00154	0.01776	$A_3 = 0$
		K_4 5.0804	5.0478 ± 0.42597	4.9978	$A_4 = 0$
		Trials = 100	av. $\sigma = 3.65\times10^{-4}$		tot. = 0
	Weighted fitting	A_1 7.26×10^{-2}	$1.07\times10^{-1} \pm 1.23\times10^{-1}$	8.02×10^{-2}	$A_1 = 0$
		A_2 1.01×10^{-3}	$4.11\times10^{-4} \pm 4.73\times10^{-4}$	4.15×10^{-5}	$A_2 = 49$
		A_3 0.0	$7.48\times10^{-6} \pm 1.95\times10^{-5}$	0.0	$A_3 = 72$
		A_4 1.20×10^{-5}	$1.70\times10^{-5} \pm 1.93\times10^{-4}$	1.22×10^{-5}	$A_4 = 0$
		Trials = 100	av. $\sigma = 6.68\times10^{-6}$		tot. = 83
	Unweighted fitting	A_1 7.26×10^{-2}	$7.27\times10^{-2} \pm 2.32\times10^{-4}$	7.27×10^{-2}	$A_1 = 0$
		A_2 1.01×10^{-3}	$9.97\times10^{-4} \pm 1.07\times10^{-5}$	9.99×10^{-4}	$A_2 = 0$
		A_3 0.0	$3.51\times10^{-7} \pm 4.33\times10^{-7}$	1.81×10^{-7}	$A_3 = 39$
		A_4 1.20×10^{-5}	$1.20\times10^{-5} \pm 1.55\times10^{-8}$	1.20×10^{-5}	$A_4 = 0$
		Trials = 100	av. $\sigma = 3.65\times10^{-4}$		
(B) 5 mM DPG, pressure noise	Weighted fitting	K_1 0.01471	0.01458 ± 0.00041	0.01458	$A_1 = 0$
		K_2 0.00887	0.00855 ± 0.00131	0.00858	$A_2 = 0$
		K_3 0.01736	0.01849 ± 0.00521	0.01875	$A_3 = 0$
		K_4 5.0804	4.9782 ± 1.1855	4.8989	$A_4 = 0$
		Trials = 100	av. $\sigma = 1.52\times10^{-5}$		tot. = 0
	Unweighted fitting	K_1 0.01471	0.01540 ± 0.00114	0.01640	$A_1 = 0$
		K_2 0.00887	0.00474 ± 0.00369	0.00429	$A_2 = 18$
		K_3 0.01736	0.07825 ± 0.07356	0.08495	$A_3 = 3$
		K_4 5.0804	2.0295 ± 1.0836	1.9411	$A_4 = 0$
		Trials = 100	av. $\sigma = 8.00\times10^{-3}$		tot. = 21
	Weighted fitting	A_1 7.26×10^{-2}	$7.25\times10^{-2} \pm 1.51\times10^{-3}$	7.23×10^{-2}	$A_1 = 0$
		A_2 1.01×10^{-3}	$9.29\times10^{-4} \pm 7.13\times10^{-5}$	9.43×10^{-4}	$A_2 = 0$
		A_3 0.0	$8.98\times10^{-7} \pm 1.05\times10^{-6}$	5.82×10^{-7}	$A_3 = 43$
		A_4 1.20×10^{-5}	$1.20\times10^{-5} \pm 1.49\times10^{-7}$	1.20×10^{-5}	$A_4 = 0$
		Trials = 100	av. $\sigma = 7.96\times10^{-6}$		tot. = 43
	Unweighted fitting	A_1 7.26×10^{-2}	$8.07\times10^{-2} \pm 9.89\times10^{-5}$	8.04×10^{-2}	$A_1 = 0$
		A_2 1.01×10^{-3}	$5.96\times10^{-4} \pm 2.36\times10^{-5}$	6.16×10^{-4}	$A_2 = 11$
		A 0.0	$1.64\times10^{-5} \pm 1.34\times10^{-5}$	1.58×10^{-5}	$A_3 = 15$
		A_4 1.20×10^{-5}	$1.21\times10^{-5} \pm 2.64\times10^{-7}$	1.21×10^{-5}	$A_4 = 0$
		Trials = 100	av. $\sigma = 8.22\times10^{-3}$		tot. = 26
(C) 5 mM DPG, absorbance + spectral noise	Weighted fitting	K_1 0.01471	0.01494 ± 0.00091	0.01491	$A_1 = 0$
		K_2 0.00887	0.00672 ± 0.00421	0.00706	$A_2 = 11$
		K_3 0.01736	0.03923 ± 0.03527	0.03302	$A_3 = 6$
		K_4 5.0804	2.9053 ± 1.8841	3.2894	$A_4 = 0$
		Trials = 100	av. $\sigma = 2.04\times10^{-5}$		tot. = 17

(continued)

Table 6 (continued)

		True	Mean ± S.D.	Median	Zeros
(**C**) 5 mM DPG, absorbance + spectral noise	Unweighted fitting	K_1 0.01471	0.01630 ± 0.00115	0.01623	$A_1 = 0$
		K_2 0.00887	0.00449 ± 0.00349	0.00415	$A_2 = 13$
		K_3 0.01736	0.07798 ± 0.07334	0.08944	$A_3 = 7$
		K_4 5.0804	2.0322 ± 1.0882	1.9210	$A_4 = 0$
		Trials = 100	av. $\sigma = 7.99 \times 10^{-3}$		tot. = 20
	Weighted fitting	A_1 7.26×10^{-2}	$1.35 \times 10^{-1} \pm 1.79 \times 10^{-1}$	8.30×10^{-2}	$A_1 = 0$
		A_2 1.01×10^{-3}	$2.78 \times 10^{-4} \pm 3.94 \times 10^{-4}$	0.0	$A_2 = 58$
		A_3 0.0	$8.95 \times 10^{-6} \pm 1.72 \times 10^{-6}$	0.0	$A_3 = 60$
		A_4 1.20×10^{-5}	$2.42 \times 10^{-5} \pm 4.37 \times 10^{-5}$	1.22×10^{-5}	$A_4 = 0$
		Trials = 100	av. $\sigma = 7.42 \times 10^{-6}$		tot. = 82
	Unweighted fitting	A_1 7.26×10^{-2}	$7.98 \times 10^{-2} \pm 5.62 \times 10^{-3}$	7.99×10^{-2}	$A_1 = 0$
		A_2 1.01×10^{-3}	$6.29 \times 10^{-4} \pm 3.80 \times 10^{-5}$	6.22×10^{-4}	$A_2 = 8$
		A_3 0.0	$1.60 \times 10^{-5} \pm 1.27 \times 10^{-5}$	1.60×10^{-5}	$A_3 = 21$
		A_4 1.20×10^{-5}	$1.21 \times 10^{-5} \pm 2.91 \times 10^{-7}$	1.21×10^{-5}	$A_4 = 0$
		Trials = 100	av. $\sigma = 8.21 \times 10^{-3}$		tot. = 29
(**D**) 5 mM IHP, absorbance noise	Weighted fitting	K_1 0.00890	0.00895 ± 0.00009	0.00894	$A_1 = 0$
		K_2 0.01147	0.01131 ± 0.00029	0.01135	$A_2 = 0$
		K_3 0.00116	0.00139 ± 0.00055	0.00134	$A_3 = 0$
		K_4 2.5376	2.1440 ± 0.84068	2.2145	$A_4 = 0$
		Trials = 100	av. $\sigma = 1.92 \times 10^{-5}$		tot. = 0
	Unweighted fitting	K_1 0.00890	0.00890 ± 0.00002	0.00891	$A_1 = 0$
		K_2 0.01147	0.01147 ± 0.00006	0.01146	$A_2 = 0$
		K_3 0.00116	0.00116 ± 0.00012	0.00117	$A_2 = 0$
		K_4 2.5376	2.5460 ± 0.25490	2.5233	$A_4 = 0$
		Trials = 100	av. $\sigma = 3.65 \times 10^{-4}$		tot. = 0
	Weighted fitting	A_1 3.44×10^{-2}	$3.46 \times 10^{-2} \pm 3.35 \times 10^{-4}$	3.46×10^{-2}	$A_1 = 0$
		A_2 6.93×10^{-4}	$6.83 \times 10^{-4} \pm 1.24 \times 10^{-5}$	6.86×10^{-4}	$A_2 = 0$
		A_3 0.0	$1.47 \times 10^{-7} \pm 1.93 \times 10^{-9}$	7.22×10^{-8}	$A_3 = 39$
		A_4 2.96×10^{-7}	$2.95 \times 10^{-5} \pm 9.85 \times 10^{-10}$	2.95×10^{-7}	$A_4 = 0$
		Trials = 100	av. $\sigma = 1.92 \times 10^{-5}$		tot. = 39
	Unweighted fitting	A_1 3.44×10^{-2}	$3.44 \times 10^{-2} \pm 6.66 \times 10^{-5}$	3.44×10^{-2}	$A_1 = 0$
		A_2 6.93×10^{-4}	$6.92 \times 10^{-4} \pm 1.65 \times 10^{-6}$	6.92×10^{-4}	$A_2 = 0$
		A_3 0.0	$1.65 \times 10^{-8} \pm 2.76 \times 10^{-8}$	2.84×10^{-9}	$A_3 = 50$
		A_4 2.96×10^{-7}	$2.96 \times 10^{-7} \pm 3.13 \times 10^{-10}$	2.96×10^{-7}	$A_4 = 0$
		Trials = 100	av. $\sigma = 3.65 \times 10^{-4}$		tot. = 50
(**E**) 5 mM IHP, pressure noise	Weighted fitting	K_1 0.00890	0.00879 ± 0.00013	0.00879	$A_1 = 0$
		K_2 0.01147	0.01135 ± 0.00056	0.01137	$A_2 = 0$
		K_3 0.00116	0.00125 ± 0.00074	0.00133	$A_3 = 9$
		K_4 2.5376	2.4072 ± 1.4164	2.2501	$A_4 = 0$
		Trials = 100	av. $\sigma = 3.95 \times 10^{-5}$		tot. = 9
	Unweighted fitting	K_1 0.00890	0.00941 ± 0.00042	0.00945	$A_1 = 0$
		K_2 0.01147	0.00974 ± 0.00124	0.00987	$A_2 = 0$
		K_3 0.00116	0.00466 ± 0.00322	0.00394	$A_3 = 7$
		K_4 2.5376	0.69361 ± 0.47344	0.80481	$A_4 = 0$
		Trials = 100	av. $\sigma = 8.62 \times 10^{-3}$		tot. = 7
	Weighted fitting	A_1 3.44×10^{-2}	$3.41 \times 10^{-2} \pm 4.93 \times 10^{-4}$	3.42×10^{-2}	$A_1 = 0$
		A_2 6.93×10^{-4}	$6.69 \times 10^{-4} \pm 2.20 \times 10^{-5}$	6.67×10^{-4}	$A_2 = 0$
		A_3 0.0	$1.29 \times 10^{-7} \pm 1.70 \times 10^{-7}$	7.12×10^{-8}	$A_3 = 44$
		A_4 2.96×10^{-7}	$2.94 \times 10^{-5} \pm 4.20 \times 10^{-9}$	2.93×10^{-7}	$A_4 = 0$
		Trials = 100	av. $\sigma = 3.78 \times 10^{-5}$		tot. = 44

(continued)

Table 6 (continued)

		True	Mean ± S.D.	Median	Zeros
(E) 5 mM IHP, pressure noise	Unweighted fitting	A_1 3.44×10^{-2}	$3.77\times10^{-2}\pm1.64\times10^{-3}$	3.69×10^{-2}	$A_1=0$
		A_2 6.93×10^{-4}	$5.48\times10^{-4}\pm6.16\times10^{-5}$	6.08×10^{-4}	$A_2=0$
		A_3 0.0	$1.26\times10^{-6}\pm1.09\times10^{-6}$	1.63×10^{-6}	$A_3=18$
		A_4 2.96×10^{-7}	$2.96\times10^{-7}\pm7.87\times10^{-9}$	2.89×10^{-7}	$A_4=0$
		Trials = 100	av. $\sigma=8.60\times10^{-3}$		tot. = 18
(F) 5 mM IHP, pressure + absorbance noise	Weighted fitting	K_1 0.00890	0.00884 ± 0.00018	0.00883	$A_1=0$
		K_2 0.01147	0.01118 ± 0.00064	0.01123	$A_2=0$
		K_3 0.00116	0.00154 ± 0.00097	0.00150	$A_3=8$
		K_4 2.5376	1.9808 ± 1.2463	2.0239	$A_4=0$
		Trials = 100	av. $\sigma=4.32\times10^{-5}$		tot. = 8
	Unweighted fitting	K_1 0.00890	0.00940 ± 0.00048	0.00935	$A_1=0$
		K_2 0.01147	0.00970 ± 0.00132	0.00974	$A_2=0$
		K_3 0.00116	0.00505 ± 0.00317	0.00505	$A_3=9$
		K_4 2.5376	0.6421 ± 0.39477	0.64429	$A_4=0$
		Trials = 100	av. $\sigma=8.66\times10^{-3}$		tot. = 9
	Weighted fitting	A_1 3.44×10^{-2}	$3.43\times10^{-2}\pm6.29\times10^{-4}$	3.42×10^{-2}	$A_1=0$
		A_2 6.93×10^{-4}	$6.64\times10^{-4}\pm2.51\times10^{-5}$	6.64×10^{-4}	$A_2=0$
		A_3 0.0	$2.39\times10^{-7}\pm2.83\times10^{-7}$	1.32×10^{-7}	$A_3=36$
		A_4 2.96×10^{-7}	$2.94\times10^{-7}\pm4.26\times10^{-9}$	2.94×10^{-7}	$A_4=0$
		Trials = 100	av. $\sigma=4.17\times10^{-5}$		tot. = 36
	Unweighted fitting	A_1 3.44×10^{-2}	$3.65\times10^{-2}\pm1.90\times10^{-3}$	3.63×10^{-2}	$A_1=0$
		A_2 6.93×10^{-4}	$6.26\times10^{-4}\pm6.52\times10^{-5}$	6.27×10^{-4}	$A_2=0$
		A_3 0.0	$1.40\times10^{-6}\pm1.05\times10^{-6}$	1.35×10^{-6}	$A_3=14$
		A_4 2.96×10^{-7}	$2.90\times10^{-7}\pm7.51\times10^{-9}$	2.90×10^{-7}	$A_4=0$
		Trials = 100	av. $\sigma=8.73\times10^{-3}$		tot. = 14

simulations of a simple tetrameric model were unable to reconstruct the comparative curve-fitting results (table 6). When data were simulated as having a positive K_3 value, then both weighted and unweighted fitting clearly resolved the positive K_3 parameter. When data were simulated as having a zero A_3 then the results were complex; a clear and consistent rationalization of the raw data from such simulations was impossible. Since none of the different kinds of tetrameric simulations were able to explain the data under the conditions of the experiment, our conclusion is that our data are more complex than the simulations would indicate, and the root cause of the parameter differences in the fitting methods is currently undetermined. It should be noted, however, that the idea that a large A_3 is a product of weighted fitting of small A_3 data can be excluded, because weighted fitting exhibited as many zero A_3 parameters as did unweighted fitting when Monte Carlo simulations with zero-valued A_3 parameters were analyzed.

4. Discussion

Because of the central position of hemoglobin as a model of cooperative interactions between subunits, there has been intensive study of the equilibrium and thermodynamic properties of hemoglobin. In the area of hemoglobin oxygenation studies, there are a number of skilled research groups, each with a special set of experimental methods, unique ways of analyzing data, and consequently different ideas about the mechanism of oxygenation. As a consequence, misunderstandings arise because of the difficulty of translating experience derived from one set of methods to other, foreign techniques. Without some attempt to compare a number of curve-fitting methods on experimental data, it is difficult to separate rationally the numerical effects from experimental results, because no common grounds exist for comparison.

The data sets we have analyzed show a clear trend, with weighted analytical methods typically yielding data with all positive parameters, or perhaps an $A_2 \approx 0$, while the majority of unweighted fittings exhibit an $A_3 = 0$. This fundamental difference demonstrates again how important it is to select carefully the procedure for analyzing data, since what seems like an arbitrary choice from some points of view (weighting, endpoints, etc.) might be critical in forming observations about hemoglobin oxygenation and thus about the functional mechanism of cooperativity.

Although the data sets we received from Gill and co-workers do not clearly exhibit these trends, the majority of data sets that showed no trends had a ΔA_t of 0.08–0.12 asorbance units. Such a value seems unusually small, considering the technique has been shown to work with ΔA_t values of 0.5 or so [17]. The values of ΔA_t obtained in our oxygen equilibrium cell average about 0.6 absorbance units. As ΔA_t falls, there is a loss of resolution due to the decreased signal-to-noise ratio, and this may well be an important factor in the size of the standard error of ΔA_t in thin-layer data observed by Marden et al. [28], typically 0.5% or more (the mean relative $\sigma_{\Delta A_t}$ of the data sets in fig. 1 was 0.059%). When data sets with larger ΔA_t were examined, four positive Adair parameters were usually obtained with weighted fitting.

Why the two types of curve fitting are different is not completely clear, because data sets with large numbers of points clearly exhibit the differences, and Monte Carlo simulations of these sets with measurement error added do not. This suggests that the perturbing factor is something other than the known instrumental error sources in the measurements, a factor we currently regard as undetermined. Dimers could be a contributor at low concentrations, but it is difficult to rationalize the concentration dependence of dimers with the concentration-independent curve-fitting differences observed over a broad concentration range *.

Another possible effector is the transformation properties of end weighting [3–9]. While end weighting of data obtained in the Imai cell is performed to counterbalance the error terms in the data [7], this weighting is equivalent to fitting the Adair equation when $\log(Y/(1-Y))$ is the dependent variable and $\log P$ is the independent variable. Consequently, the end weights transform a fit of Y vs $[O_2]$ to an equally weighted fit on the Hill plot. This transformation may turn out to be the most significant characteristic of end-weighted fitting, since it preserves a correlation between fitted Adair parameters and their asymptotic, unity slope representation in the Hill domain. Consistent with this interpretation would be the notion that equally weighted fitting of the tetrameric Adair equation has insufficient resolution to resolve the upper asymptotic parameters. This loss of resolution would not yield an $A_4 = 0$, since $A_4 = P_m^{-4}$ and thus A_4 is determined by the overall shape and position of the curve. A_3, however, is the most sensitive parameter to the upper asymptote of the Hill plot. As a consequence, we believe that inability to resolve the asymptote creates a condition where small A_3 results are observed. Although the merits of end weighting are currently a matter under debate [10,27,31,32], we believe that all data should be properly weighted, with the weighting coming from an experimentally determined σ_Y vs Y graph **. For the Imai cell, end weighting is clearly the preferred weighting technique [5].

---

* One should not underestimate the contributions of dimers in other subtle ways, however. If A_3 were truly zero, then while dimers are almost absent at millimolar total hemoglobin concentrations, the dimeric equivalent of the triply bound species carries enough oxygen load that the upper asymptote of the Hill plot has a slope of unity. Simulations using the fitted parameters of data set C of Mills et al. [29], with A_3 set to zero, suggest that this is true throughout the measurable concentration range (i.e., to at least 50 mM) of oxygen equilibrium curves [30].

** A residual plot is insufficient because a residual vector is defined relative to a single data set and thus lacks the data set-to-data set comparisons needed to delineate properly a σ_Y vs Y graph.

Because many common HbA results are currently in dispute, other conditions or other compounds which simplify the data analysis should be pursued. One approach would be to examine HbA under conditions where cooperativity is very low, perhaps 2.0, as in the data sets of Poyart. Another possibility is suggested by the lack of $A_3 = 0$ results in cobalt hemoglobin. Cobalt hemoglobin is useful because it can serve as a control for data analysis algorithms. Questions such as the effects of endpoints on parameters and parameter resolution would be usefully approached with cobalt hemoglobin studies. By analyzing cobalt hemoglobin data taken under a variety of conditions with a spectrum of experimental techniques, it should be possible to create a body of data through which all data analysis methods can be directly compared.

Appendix A: List of the oxygen partial pressures and Y values for the IHP data set of fig. 1

Pt.	p_{O_2}	Y	Pt.	p_{O_2}	Y
1.	0.35350E +0	0.38837E −2	41.	0.96744E +0	0.99087E −2
2.	0.36393E +0	0.43267E −2	42.	0.99351E +0	0.10174E −1
3.	0.37137E +0	0.44152E −2	43.	0.10138E +1	0.99530E −2
4.	0.38143E +0	0.43660E −2	44.	0.10417E +1	0.10145E −1
5.	0.38962E +0	0.43858E −2	45.	0.10733E +1	0.10809E −1
6.	0.39855E +0	0.34456E −2	46.	0.10960E +1	0.10809E −1
7.	0.40730E +0	0.38097E −2	47.	0.11264E +1	0.10903E −1
8.	0.41587E +0	0.41396E −2	48.	0.11509E +1	0.11754E −1
9.	0.42555E +0	0.48878E −2	49.	0.11802E +1	0.11257E −1
10.	0.44323E +0	0.45729E −2	50.	0.12195E +1	0.11887E −1
11.	0.46073E +0	0.49223E −2	51.	0.12524E +1	0.12286E −1
12.	0.47171E +0	0.46959E −2	52.	0.12829E +1	0.12227E −1
13.	0.48567E +0	0.48977E −2	53.	0.13099E +1	0.12793E −1
14.	0.49684E +0	0.48977E −2	54.	0.13380E +1	0.13270E −1
15.	0.50764E +0	0.53898E −2	55.	0.13715E +1	0.12921E −1
16.	0.51825E +0	0.55721E −2	56.	0.14097E +1	0.13192E −1
17.	0.52961E +0	0.53949E −2	57.	0.14412E +1	0.13654E −1
18.	0.54748E +0	0.53949E −2	58.	0.14728E +1	0.14225E −1
19.	0.56014E +0	0.58576E −2	59.	0.15032E +1	0.13777E −1
20.	0.57819E +0	0.60052E −2	60.	0.15342E +1	0.14255E −1
21.	0.59290E +0	0.58919E −2	61.	0.15674E +1	0.14220E −1
22.	0.61152E +0	0.63546E −2	62.	0.16165E +1	0.15234E −1
23.	0.62492E +0	0.63843E −2	63.	0.16567E +1	0.15732E −1
24.	0.63814E +0	0.69700E −2	64.	0.16927E +1	0.16219E −1
25.	0.65638E +0	0.68815E −2	65.	0.17293E +1	0.16224E −1
26.	0.67518E +0	0.66944E −2	66.	0.17751E +1	0.16716E −1
27.	0.68970E +0	0.72752E −2	67.	0.18161E +1	0.16721E −1
28.	0.70906E +0	0.78216E −2	68.	0.18613E +1	0.17676E −1
29.	0.72749E +0	0.73638E −2	69.	0.19004E +1	0.17553E −1
30.	0.75020E +0	0.73884E −2	70.	0.19460E +1	0.18163E −1
31.	0.76714E +0	0.80334E −2	71.	0.19862E +1	0.18193E −1
32.	0.78390E +0	0.82793E −2	72.	0.20268E +1	0.18680E −1
33.	0.80084E +0	0.81465E −2	73.	0.20743E +1	0.19438E −1
34.	0.81815E +0	0.79644E −2	74.	0.21173E +1	0.20147E −1
35.	0.83714E +0	0.84025E −2	75.	0.21633E +1	0.19985E −1
36.	0.86301E +0	0.87175E −2	76.	0.22085E +1	0.20501E −1
37.	0.88665E +0	0.91754E −2	77.	0.22562E +1	0.20467E −1
38.	0.90620E +0	0.93328E −2	78.	0.23025E +1	0.20989E −1
39.	0.92798E +0	0.90620E −2	79.	0.23552E +1	0.21643E −1
40.	0.94697E +0	0.98693E −2	80.	0.24114E +1	0.22303E −1

(continued)

Appendix A (continued)

Pt.	P_{O_2}	Y	Pt.	P_{O_2}	Y
81.	0.24676E+1	0.22544E−1	134.	0.76022E+1	0.65744E−1
82.	0.25201E+1	0.22648E−1	135.	0.77650E+1	0.66925E−1
83.	0.25735E+1	0.23032E−1	136.	0.79356E+1	0.67836E−1
84.	0.26283E+1	0.24095E−1	137.	0.80986E+1	0.69889E−1
85.	0.26843E+1	0.24287E−1	138.	0.82643E+1	0.71341E−1
86.	0.27415E+1	0.24641E−1	139.	0.84432E+1	0.72985E−1
87.	0.27999E+1	0.25655E−1	140.	0.86158E+1	0.73812E−1
88.	0.28586E+1	0.25429E−1	141.	0.87977E+1	0.75333E−1
89.	0.29207E+1	0.26084E−1	142.	0.89877E+1	0.77967E−1
90.	0.29850E+1	0.26586E−1	143.	0.91811E+1	0.79709E−1
91.	0.30544E+1	0.26950E−1	144.	0.93701E+1	0.80955E−1
92.	0.31259E+1	0.27624E−1	145.	0.95652E+1	0.82776E−1
93.	0.31951E+1	0.28186E−1	146.	0.97604E+1	0.84632E−1
94.	0.32623E+1	0.29032E−1	147.	0.99702E+1	0.86561E−1
95.	0.33351E+1	0.29938E−1	148.	0.10177E+2	0.87772E−1
96.	0.34081E+1	0.30499E−1	149.	0.10393E+2	0.90100E−1
97.	0.34803E+1	0.30922E−1	150.	0.10614E+2	0.92030E−1
98.	0.35518E+1	0.31336E−1	151.	0.10835E+2	0.93581E−1
99.	0.36294E+1	0.31973E−1	152.	0.11058E+2	0.95476E−1
100.	0.37070E+1	0.32793E−1	153.	0.11284E+2	0.97952E−1
101.	0.38037E+1	0.32896E−1	154.	0.11517E+2	0.99876E−1
102.	0.38863E+1	0.33457E−1	155.	0.11755E+2	0.10238E+0
103.	0.39665E+1	0.34166E−1	156.	0.12007E+2	0.10498E+0
104.	0.40559E+1	0.35367E−1	157.	0.12265E+2	0.10683E+0
105.	0.41406E+1	0.36756E−1	158.	0.12520E+2	0.10913E+0
106.	0.42344E+1	0.36869E−1	159.	0.12780E+2	0.11142E+0
107.	0.43210E+1	0.37513E−1	160.	0.13050E+2	0.11408E+0
108.	0.44152E+1	0.38380E−1	161.	0.13322E+2	0.11616E+0
109.	0.45083E+1	0.39389E−1	162.	0.13594E+2	0.11885E+0
110.	0.46030E+1	0.40310E−1	163.	0.13873E+2	0.12107E+0
111.	0.46985E+1	0.40718E−1	164.	0.14158E+2	0.12402E+0
112.	0.47953E+1	0.41328E−1	165.	0.14453E+2	0.12721E+0
113.	0.48992E+1	0.42347E−1	166.	0.14760E+2	0.12904E+0
114.	0.50045E+1	0.44060E−1	167.	0.15072E+2	0.13238E+0
115.	0.51094E+1	0.44764E−1	168.	0.15381E+2	0.13542E+0
116.	0.52199E+1	0.45168E−1	169.	0.15696E+2	0.13838E+0
117.	0.53340E+1	0.46256E−1	170.	0.16031E+2	0.14138E+0
118.	0.54495E+1	0.47226E−1	171.	0.16359E+2	0.14469E+0
119.	0.55638E+1	0.48200E−1	172.	0.16697E+2	0.14769E+0
120.	0.56775E+1	0.49643E−1	173.	0.17043E+2	0.15145E+0
121.	0.57961E+1	0.49874E−1	174.	0.17392E+2	0.15496E+0
122.	0.59160E+1	0.51429E−1	175.	0.17750E+2	0.15755E+0
123.	0.60453E+1	0.52606E−1	176.	0.18113E+2	0.16161E+0
124.	0.61693E+1	0.53640E−1	177.	0.18486E+2	0.16473E+0
125.	0.63006E+1	0.54595E−1	178.	0.18864E+2	0.16803E+0
126.	0.64318E+1	0.55623E−1	179.	0.19255E+2	0.17272E+0
127.	0.65643E+1	0.56706E−1	180.	0.19657E+2	0.17680E+0
128.	0.66987E+1	0.57873E−1	181.	0.20074E+2	0.18058E+0
129.	0.68397E+1	0.58912E−1	182.	0.20486E+2	0.18479E+0
130.	0.69804E+1	0.60044E−1	183.	0.20904E+2	0.18829E+0
131.	0.71275E+1	0.61516E−1	184.	0.21340E+2	0.19343E+0
132.	0.72803E+1	0.62707E−1	185.	0.21780E+2	0.19665E+0
133.	0.74402E+1	0.63992E−1	186.	0.22232E+2	0.20176E+0

(continued)

Appendix A (continued)

Pt.	p_{O_2}	Y	Pt.	p_{O_2}	Y
187.	0.22692*E* +2	0.20678*E* +0	240.	0.67049*E* +2	0.65086*E* +0
188.	0.23158*E* +2	0.21067*E* +0	241.	0.68427*E* +2	0.66167*E* +0
189.	0.23633*E* +2	0.21567*E* +0	242.	0.69834*E* +2	0.67150*E* +0
190.	0.24133*E* +2	0.22144*E* +0	243.	0.71271*E* +2	0.68266*E* +0
191.	0.24626*E* +2	0.22703*E* +0	244.	0.72737*E* +2	0.69158*E* +0
192.	0.25134*E* +2	0.23182*E* +0	245.	0.74224*E* +2	0.70147*E* +0
193.	0.25650*E* +2	0.23676*E* +0	246.	0.75763*E* +2	0.71090*E* +0
194.	0.26176*E* +2	0.24178*E* +0	247.	0.77332*E* +2	0.72191*E* +0
195.	0.26723*E* +2	0.24766*E* +0	248.	0.78911*E* +2	0.73139*E* +0
196.	0.27291*E* +2	0.25448*E* +0	249.	0.80533*E* +2	0.74021*E* +0
197.	0.27861*E* +2	0.25988*E* +0	250.	0.82183*E* +2	0.75139*E* +0
198.	0.28442*E* +2	0.26625*E* +0	251.	0.83882*E* +2	0.76132*E* +0
199.	0.29027*E* +2	0.27170*E* +0	252.	0.85616*E* +2	0.77005*E* +0
200.	0.29624*E* +2	0.27906*E* +0	253.	0.87374*E* +2	0.77770*E* +0
201.	0.30234*E* +2	0.28547*E* +0	254.	0.89161*E* +2	0.78854*E* +0
202.	0.30855*E* +2	0.29244*E* +0	255.	0.91045*E* +2	0.79555*E* +0
203.	0.31493*E* +2	0.29926*E* +0	256.	0.92905*E* +2	0.80417*E* +0
204.	0.32137*E* +2	0.30654*E* +0	257.	0.94812*E* +2	0.81276*E* +0
205.	0.32801*E* +2	0.31405*E* +0	258.	0.96760*E* +2	0.81951*E* +0
206.	0.33472*E* +2	0.32188*E* +0	259.	0.98737*E* +2	0.82635*E* +0
207.	0.34165*E* +2	0.32878*E* +0	260.	0.10077*E* +3	0.83471*E* +0
208.	0.34863*E* +2	0.33617*E* +0	261.	0.10286*E* +3	0.84109*E* +0
209.	0.35586*E* +2	0.34406*E* +0	262.	0.10497*E* +3	0.84764*E* +0
210.	0.36317*E* +2	0.35238*E* +0	263.	0.10712*E* +3	0.85416*E* +0
211.	0.37061*E* +2	0.35989*E* +0	264.	0.10931*E* +3	0.86032*E* +0
212.	0.37818*E* +2	0.36819*E* +0	265.	0.11155*E* +3	0.86627*E* +0
213.	0.38597*E* +2	0.37706*E* +0	266.	0.11386*E* +3	0.87219*E* +0
214.	0.39392*E* +2	0.38588*E* +0	267.	0.11621*E* +3	0.87814*E* +0
215.	0.40209*E* +2	0.39451*E* +0	268.	0.11861*E* +3	0.88258*E* +0
216.	0.41053*E* +2	0.40325*E* +0	269.	0.12106*E* +3	0.88786*E* +0
217.	0.41893*E* +2	0.41255*E* +0	270.	0.12356*E* +3	0.89317*E* +0
218.	0.42754*E* +2	0.42235*E* +0	271.	0.12613*E* +3	0.89860*E* +0
219.	0.43646*E* +2	0.43119*E* +0	272.	0.12873*E* +3	0.90264*E* +0
220.	0.44545*E* +2	0.44149*E* +0	273.	0.13144*E* +3	0.90719*E* +0
221.	0.45462*E* +2	0.45014*E* +0	274.	0.13414*E* +3	0.91152*E* +0
222.	0.46399*E* +2	0.46022*E* +0	275.	0.13691*E* +3	0.91535*E* +0
223.	0.47357*E* +2	0.46961*E* +0	276.	0.13972*E* +3	0.91885*E* +0
224.	0.48349*E* +2	0.48015*E* +0	277.	0.14259*E* +3	0.92182*E* +0
225.	0.49377*E* +2	0.49087*E* +0	278.	0.14552*E* +3	0.92545*E* +0
226.	0.50385*E* +2	0.50212*E* +0	279.	0.14855*E* +3	0.92972*E* +0
227.	0.51428*E* +2	0.51241*E* +0	280.	0.15168*E* +3	0.93209*E* +0
228.	0.52491*E* +2	0.52335*E* +0	281.	0.15485*E* +3	0.93461*E* +0
229.	0.53593*E* +2	0.53365*E* +0	282.	0.15806*E* +3	0.93851*E* +0
230.	0.54698*E* +2	0.54432*E* +0	283.	0.16137*E* +3	0.94092*E* +0
231.	0.55817*E* +2	0.55543*E* +0	284.	0.16472*E* +3	0.94298*E* +0
232.	0.56964*E* +2	0.56456*E* +0	285.	0.16809*E* +3	0.94647*E* +0
233.	0.58130*E* +2	0.57735*E* +0	286.	0.17154*E* +3	0.94794*E* +0
234.	0.59321*E* +2	0.58621*E* +0	287.	0.17504*E* +3	0.95068*E* +0
235.	0.60532*E* +2	0.59811*E* +0	288.	0.17863*E* +3	0.95234*E* +0
236.	0.61772*E* +2	0.60829*E* +0	289.	0.18228*E* +3	0.95481*E* +0
237.	0.63051*E* +2	0.61949*E* +0	290.	0.18605*E* +3	0.95614*E* +0
238.	0.64349*E* +2	0.62958*E* +0	291.	0.18987*E* +3	0.95903*E* +0
239.	0.65674*E* +2	0.64016*E* +0	292.	0.19382*E* +3	0.96037*E* +0

(continued)

Appendix A (continued)

Pt.	P_{O_2}	Y	Pt.	P_{O_2}	Y
293.	0.19780*E* +3	0.96210*E* +0	326.	0.38737*E* +3	0.99014*E* +0
294.	0.20185*E* +3	0.96315*E* +0	327.	0.39533*E* +3	0.99037*E* +0
295.	0.20602*E* +3	0.96549*E* +0	328.	0.40359*E* +3	0.99028*E* +0
296.	0.21025*E* +3	0.96726*E* +0	329.	0.41193*E* +3	0.99094*E* +0
297.	0.21458*E* +3	0.96876*E* +0	330.	0.42047*E* +3	0.99097*E* +0
298.	0.21897*E* +3	0.96926*E* +0	331.	0.42920*E* +3	0.99177*E* +0
299.	0.22346*E* +3	0.97061*E* +0	332.	0.43814*E* +3	0.99179*E* +0
300.	0.22806*E* +3	0.97192*E* +0	333.	0.44712*E* +3	0.99221*E* +0
301.	0.23277*E* +3	0.97287*E* +0	334.	0.45640*E* +3	0.99195*E* +0
302.	0.23755*E* +3	0.97418*E* +0	335.	0.46593*E* +3	0.99272*E* +0
303.	0.24250*E* +3	0.97514*E* +0	336.	0.47550*E* +3	0.99361*E* +0
304.	0.24750*E* +3	0.97613*E* +0	337.	0.48521*E* +3	0.99275*E* +0
305.	0.25257*E* +3	0.97749*E* +0	338.	0.49512*E* +3	0.99372*E* +0
306.	0.25782*E* +3	0.97757*E* +0	339.	0.50547*E* +3	0.99380*E* +0
307.	0.26312*E* +3	0.97891*E* +0	340.	0.51586*E* +3	0.99397*E* +0
308.	0.26853*E* +3	0.97999*E* +0	341.	0.52662*E* +3	0.99383*E* +0
309.	0.27407*E* +3	0.98036*E* +0	342.	0.53746*E* +3	0.99458*E* +0
310.	0.27970*E* +3	0.98135*E* +0	343.	0.54845*E* +3	0.99507*E* +0
311.	0.28541*E* +3	0.98198*E* +0	344.	0.55983*E* +3	0.99475*E* +0
312.	0.29135*E* +3	0.98284*E* +0	345.	0.57143*E* +3	0.99493*E* +0
313.	0.29732*E* +3	0.98349*E* +0	346.	0.58311*E* +3	0.99516*E* +0
314.	0.30339*E* +3	0.98384*E* +0	347.	0.59504*E* +3	0.99533*E* +0
315.	0.30961*E* +3	0.98478*E* +0	348.	0.60739*E* +3	0.99565*E* +0
316.	0.31594*E* +3	0.98538*E* +0	349.	0.61984*E* +3	0.99576*E* +0
317.	0.32240*E* +3	0.98580*E* +0	350.	0.63263*E* +3	0.99615*E* +0
318.	0.32908*E* +3	0.98664*E* +0	351.	0.64561*E* +3	0.99609*E* +0
319.	0.33583*E* +3	0.98650*E* +0	352.	0.65880*E* +3	0.99610*E* +0
320.	0.34273*E* +3	0.98730*E* +0	353.	0.67249*E* +3	0.99616*E* +0
321.	0.34981*E* +3	0.98746*E* +0	354.	0.68655*E* +3	0.99664*E* +0
322.	0.35702*E* +3	0.98833*E* +0	355.	0.70061*E* +3	0.99629*E* +0
323.	0.36442*E* +3	0.98878*E* +0	356.	0.71495*E* +3	0.99637*E* +0
324.	0.37191*E* +3	0.98911*E* +0	357.	0.72967*E* +3	0.99668*E* +0
325.	0.37960*E* +3	0.98964*E* +0	358.	0.74482*E* +3	0.99706*E* +0

Acknowledgements

We would like to thank all those who lent us their time, their encouragement, and their data sets, including Professor Gary Ackers and Professor Michael Johnson, Motoyasu Fujii, Dr Kim Vandegriff and Professor Robert Winslow, Professor Claude Poyart, Professor Stanley Gill and Dr Michael Doyle. Without the cooperation of these people, our work would be considerably less complete. We would also like to thank Dr Kim Vandegriff, Professor Michael Johnson, Professor Stanley Gill and Professor Gary Ackers for helpful suggestions with the manuscript.

References

1 G.S. Adair, Proc. Roy. Soc. Lond. A109 (1925) 292.
2 G.S. Adair, J. Biol. Chem. 63 (1925) 529.
3 F.J.W. Roughton, A.B. Otis and R.J.L. Lyster, Proc. Roy. Soc. Lond. B144 (1955) 29.
4 K. Imai, Arch. Biochem. Biophys. 127 (1968) 543.
5 K. Imai, Biochemistry 12 (1973) 798.
6 K. Imai, Methods Enzymol. 76 (1981) 470.
7 K. Imai, Allosteric effects in hemoglobin (Cambridge University Press, Cambridge, U.K., 1982).
8 K. Imai, H. Morimoto, M. Kotani, H. Watari, W. Hirata and M. Kuroda, Biochim. Biophys. Acta 200 (1970) 189.
9 K. Imai and T. Yonetani, Biochim. Biophys. Acta 490 (1977) 164.
10 S.J. Gill, E. Di Cera, M. Doyle, G.A. Bishop and C.H. Robert, Biochemistry 26 (1987) 3995.

11 S.J. Gill, P.R. Connelly, E. Di Cera and C.H. Robert, Biophys. Chem. 30 (1988) 133.
12 E. Di Cera and S.J. Gill, Biophys. Chem. 29 (1988) 351.
13 E. Di Cera and S.J. Gill, Biophys. Chem. 32 (1988) 149.
14 E. Di Cera, C.H. Robert and S.J. Gill, Biochemistry 26 (1987) 4003.
15 M.L. Doyle, E. Di Cera, C.H. Robert and S.J. Gill, J. Mol. Biol. 196 (1987) 927.
16 M.L. Doyle, E. Di Cera and S.J. Gill, Biochemistry 27 (1988) 820.
17 D. Dolman and S.J. Gill, Anal. Biochem. 87 (1978) 127.
18 K. Imaizumi, K. Imai and I. Tyuma, J. Biochem. (Tokyo) 86 (1979) 1829.
19 E. Di Cera, F.A. Bassi and S.J. Gill, Biophys. Chem. 34 (1989) 19.
20 A. Hayashi, T. Suzuki and M. Shin, Biochim. Biophys. Acta 310 (1973) 309.
21 J.E. Dennis, D.M. Gay and R.E. Welsch, ACM Trans. Math. Softw. 7 (1981) 369.
22 D.M. Gay, ACM Trans. Math. Softw. 9 (1983) 503.
23 W.H. Press, B.P. Flannery, S.A. Teukolsky and W.T. Vetterling, Numerical recipes: The art of scientific computing (Cambridge University Press, Cambridge, U.K., 1986) p. 529.
24 Cary 118 spectrophotometer instruction manual (Varian Instrument Division, Palo Alto, CA, 1972).
25 K.V. Vandegriff, F. Medina, M.A. Marini and R.M. Winslow, J. Biol. Chem. 264 (1989) 17824.
26 K.V. Vandegriff, F. Medina and R.M. Winslow, in: Symposium on oxygen binding heme proteins: Structure, dynamics, function and genetics, Asilomar Conference Grounds, Pacific Grove, CA (1988).
27 A.H. Chu, B.W. Turner and G.K. Ackers, Biochemistry 23 (1984) 604.
28 M.C. Marden, J. Kister, C. Poyart and S.J. Edelstein, J. Mol. Biol. 208 (1989) 341.
29 F.C. Mills and G.K. Ackers, J. Biol. Chem. 254 (1979) 2881.
30 F.C. Mills, Ph.D. thesis, University of Virginia, University Microfilms 79-03527 (1978).
31 F.C. Mills, M.L. Johnson and G.K. Ackers, Biochemistry 15 (1976) 5350.
32 M.L. Johnson and G.K. Ackers, Biophys. Chem. 7 (1977) 77.